JOURNAL OF MATERIALS SCIENCE 31 (1996) 4503–4519

Microstructural dependence of fracture energy and toughness of ceramics and ceramic composites versus that of their tensile strengths at 22 °C

R. W. RICE
5411 Hopark Drive, Alexandria, VA 22310, USA

The microstructural dependence of fracture energy and toughness of ceramics and ceramic particulate, platelet, and whisker composites is compared with the corresponding dependence of their tensile (flexure) strengths at 22 °C. These comparisons show that fracture energy and toughness often do not have the same porosity, or grain- or particle-size dependence as strength. This is attributed to the scale of the cracks for measuring fracture energy or toughness often being too large in comparison to the cracks controlling strength. The large cracks reflect crack–microstructure interaction phenomena such as crack-wake bridging and *R*-curve effects that are not, or are much less, involved in the control of propagation of most strength-controlling cracks. Thus fracture mechanics must account for the scale of the cracks used in measuring fracture mechanics parameters relative to the scale of the cracks controlling the strength behaviour that is to be explained or predicted.

1. Introduction

Fracture mechanics has appropriately become the method for addressing strength and failure of ceramics, but still leaves important questions of differences between different fracture mechanics tests [1] and strength tests. The focus on crack-wake effects of transformation toughening, and especially crack bridging (because of its broader applicability) and their associated *R*-curve effects, driven by the belief that toughening was the route to higher ceramic reliability [2, 3], has heightened some of these questions, especially of crack size. The question of the applicability of observations of bridging-wake effects, and related *R*-curve effects is accentuated by the large scale of cracks for such studies in comparison with those controlling normal strength [4]. The questions of crack-size effects are, in turn, related to the question of whether increased toughness increases reliability [5–7]. An important, but seriously neglected, step in resolving these issues is to compare the microstructural dependences of strength and fracture energy and toughness because this allows a much broader range of data to be more effectively evaluated.

This paper presents such a microstructural–property comparison, primarily at 22 °C, drawing on reviews of the grain-size and porosity dependence of fracture energy and toughness of ceramics [1, 8–10], the corresponding dependence of tensile (flexure) strength [11–18], and of fracture mode [19]. A similar comparison is made for ceramic particulate composites based on a review of their strength and toughness dependence [6], along with similar observations on platelet and whisker composites as a function of the dispersed phase. The issue is not the validity of fracture mechanics, but the correct application of it. In particular, phenomena seen with larger scale cracks may not be pertinent to much strength behaviour, except in cases of severe damage and resultant large cracks. This is consistent with earlier studies showing crack-size dependences of fracture mechanics parameters [20–23].

2. Comparison of ceramic microstructural dependence of fracture energy, toughness and strength

2.1. Grain-size dependence of ceramics

2.1.1. Summary of the grain-size dependence of fracture energy and toughness

An earlier review of the grain-size, G, dependence of fracture energy, γ, primarily of oxides, showed little or no G dependence for cubic materials [1, 9, 10]. A more recent survey [1] is not inconsistent with the earlier data, but shows (usually) modest toughness maxima as a function of G is common, but not necessarily universal, for cubic oxides and non-oxides. (Such K^* maxima are less pronounced than for γ, because $K_{IC} \simeq (E\gamma)^{1/2}$, and E normally has no dependence on G). Some data differ on the G location of the maxima, the magnitude of the maximum toughness, or

* Note that because there is uncertainty in which values of fracture energy or toughness are the critical ones, e.g. K_{IC}, the written terms or the symbols γ and K will be used, respectively. Only where there is reasonable certainty that a value was critical will the subscript IC be used.

0022–2461

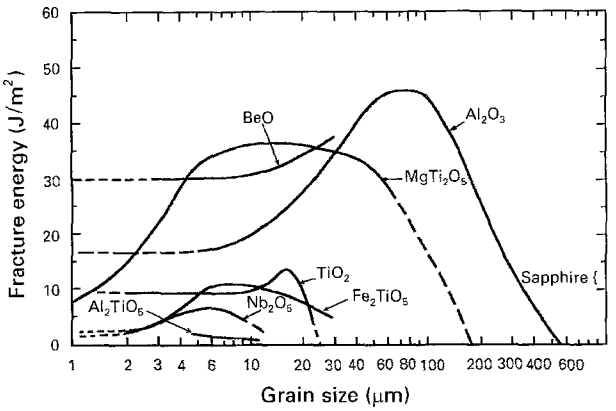

Figure 1 Summary of ceramic fracture toughness versus grain size at 22 °C.

both. Both differences depend on the test, but the G location of the K maximum also can depend considerably on the G measurement method. There was also considerable consistency of data, with K values from fractography (i.e. calculated from the failure stress and the size, shape and location of the failure-causing flaw), but these were often somewhat lower. Substantially lower toughness was found for MgO and $MgAl_2O_4$ with residual LiF additive at the grain boundaries, and resultant intergranular fracture (favouring bridging), in contrast to normal predominately transgranular fracture in these materials.

The earlier review showed significant γ maxima for non-cubic oxides [9, 10]. A subsequent survey [1] generally confirmed corresponding K maxima at $G \simeq 50$–100 μm for Al_2O_3, (Fig. 1) and associated this with R-curve effects and microcracking from thermal expansion anisotropy (TEA) between the grains. Variations in the extent to which R-curve effects occurred with different tests was seen as an important factor in test differences. In the absence of R-curve effects in Al_2O_3, γ and K appear to be independent of G over the range studied ($G \simeq 1$–30 μm), with $K \simeq 4$ MPa m$^{1/2}$, which is also obtained from fractography. A significant exception was some work of fracture (WOF) data showing a K maxima for alumina at a much finer G range (~ 15 μm) [24] than would be expected for cracking from TEA. While the K levels of one TiO_2 study were about twice those of two other studies, all three studies were consistent with a maximum, or at least a significant decrease in γ or K at $G \simeq 15$ μm, also associated with microcracking [1]. However, data for B_4C, which has very similar E and TEA to that of Al_2O_3, also showed a K maxima, similar in relative height and in absolute values to that for most alumina data, but probably narrower, and clearly at a much finer G, i.e. at $G \simeq 5$–10 μm. Again, the lower K levels from various tests were consistent with K values from fractography. TiB_2 data showed a continuous decrease in toughness from the finest G (~ 1–2 μm), suggesting a maxima there or at finer G, which is too fine a G range for this to be associated with cracking, despite its greater TEA.

The review summarized above shows four common trends central to this paper: (1) the common occurrence of γ and K maxima as a function of G (Fig. 1) or a decrease at larger G (whether or not maxima are observed at finer G), (2) values of K or γ calculated from fractography data being consistent with the lower values from other tests, i.e. in the absence of maxima, R-curve effects, etc., (3) the decreasing K at large G being consistent with an expected transition to single crystal (e.g. ~ 1–2 MPa m$^{1/2}$) and bicrystal toughness (but is probably dependent on the test) for both cubic and non-cubic materials, and (4) while there is considerable consistency of values, and especially trends, between tests, there are still significant discrepancies in both γ and K levels and their G dependence, that present problems in the application of fracture mechanics and require further test evaluation and development.

2.1.2. Summary of the grain-size dependence of tensile (flexure) strength

Despite variations due to measurement issues of both tensile strength, S and G and differing material character, previous reviews [11–14] show there is a remarkably consistent S–G pattern (easiest seen and typically shown for bodies of little porosity and variations of it, usually $P \simeq 0\%$, Fig. 2) that is central to the evaluations in this paper. There are four basic aspects to this S–G pattern: (1) a finer G regime of one or more

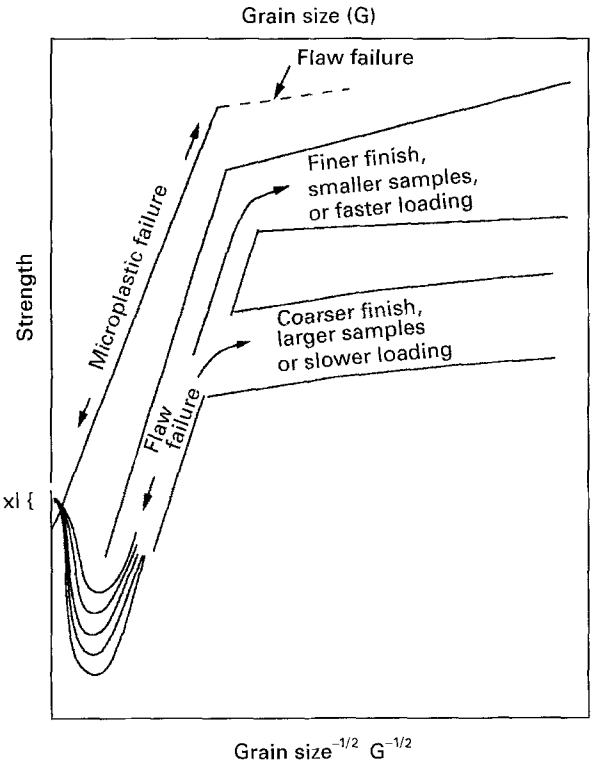

Figure 2 Summary of ceramic tensile strength as a function of grain size. Two types of behaviour are shown. The lower, branched behaviour is for failure controlled by pre-existing flaws, and shows the transition to single-crystal strengths. The upper line intersecting the strength axis at the single-crystal strength reflects failure controlled by slip or twin-crack nucleation or growth, which may change over to flaw failure at finer grain size as shown. These forms of behaviour are pertinent to bodies whose character is constant, except for grain size, and remarkably consistent over a broad range of materials, preparation, and test-temperature conditions.

S levels (i.e. branches) where there is almost always some, but limited, and occasionally no, S decrease with increasing G, (2) a larger G regime (single branch) with substantial G dependence of S, (3) the intersection of the finer and larger G branch(es) when $G \simeq$ the flaw size, C, and (4) the transition from larger G strengths to those for bi and single crystals.

Such two-branched S–G behaviour was first emphasized by Carniglia [25]. However, he identified the finer G branch as being determined by microplastic-controlled tensile (flexure) strengths of Al_2O_3, BeO, and MgO, and the larger G branch as being due to failure from flaws whose size was G. Rice [12, 26], subsequently showed directly by fractography that (1) both branches were typically due to failure from machining flaws in machined specimens, which are by far the most common specimens used (and reflective of many components), and (2) this two-branched behaviour results from the flaw depth (i.e. typically the flaw size, C) from a given machining operation not varying much with G; i.e. similar for single and polycrystalline specimens of the same material. (Flaw shape is determined mainly by the direction of machining relative to the subsequent tensile axis, and so does not vary much, except when C and G are similar [27].) Thus, at finer G the machining flaws causing failure are much larger than the grains. As G increases there is typically some limited reduction in strength due to such factors as some limited increase in C, and more opportunity for contributions of stresses from TEA in non-cubic materials and elastic anisotropy (EA) in all crystalline materials. Variability in flaw populations results in a wider scatter in the finer G branch, or multiple finer grain branches, depending on whether the specimen populations reflecting the different flaw populations can be adequately identified, e.g. as they can for machining specimens parallel or perpendicular to the subsequent tensile axis [27]. The variations in strength, which are, of course, proportional to $C^{-1/2}$, result in corresponding shifts in the intersection of the larger and finer G branches (unless there is a shift in the flaw character with increasing G, as is the case for specimens machined perpendicular to the tensile axis [27]).

The larger grain branch reflects the region where $C < G$; a natural consequence of the nearly constant flaw size. Thus, a grain size is reached beyond which C becomes progressively $< G$ as G increases. The more pronounced G dependence of S in the large G branch results from the size of the grain containing the flaw becoming the upper limit of the flaw size due to crack growth. Because $C \leqslant G$ there is only one large G branch. Flaw variations have only a secondary effect on strength variations in the larger G branch because G sets an upper limit on C. Flaw variations simply determine the G, and hence the S, level at which the finer and larger G branches intersect. Flaw growth within a single grain has been modelled, and the resulting prediction of a S–$G^{-1/2}$ slope being less than the polycrystalline K_{IC} [28–30] has been corroborated [13, 14]. A key aspect of the larger G branch is that as G increases, S extends to levels well below those for the weakest orientation of single crystals of the same material with the same machining (and hence approximately the same C). This is attributed to contributions of TEA and EA to failure and to increasing grain-boundary failure. As G is further increased, flaws become further removed from surrounding grain boundaries, reducing, then eliminating, the effects causing the decrease of S, so it reverses its downward trend with increasing G and transition to single-crystal strengths. Also as G becomes very large, the opportunity for failure from flaws along grain boundaries is reduced. However, the rate of this reduction should be quite dependent on the specimen size and the type of test. Thus in testing with a significant stress gradients, e.g. as in flexure, flaws at grain boundaries will generally have less opportunity to be activated as G approaches and then exceeds the specimen dimensions than for true tensile testing. However, both must have such a transition, though at different rates as a function of G and of specimen size.

Because the finer G branch reflects $C > G$, and the larger grain branch $C < G$, the two branches meet when $G \sim C$. This intersection is only approximately at $G \sim C$ due to some variations of C, G, the orientation of the grain and the flaw relative to the stress axis, and of the contributions of TEA and EA to the failure stress. A particularly important variable is the location of the failure-causing flaw relative to the grain, in particular whether the flaw is on a grain boundary or in the grain. In the former case, whether it lies along one or more boundary facets (hence impacting flaw geometry) should be important. Variable location of flaws within the grain is commonly observed (e.g. a flaw adjacent to, or straddling, a grain boundary) has somewhat different effects on strength than a flaw not initially abutting any grain boundary.

The above S–G behaviour has been widely observed for machined samples. Thus, the two-branched behaviour has been demonstrated extensively for flexure strengths and to also be valid for diametral compression, hoop tensile, and true tensile testing [14]. It has also been shown to hold over a broad range of test temperatures, e.g. from -196 to $> 1200\,^{\circ}C$, so long as normal brittle fracture from flaws is occurring [15], and processes such as creep are not significant. The same two-branched behaviour has also been shown to occur for specimens tested with as-fired surfaces. For such specimens, the G dependence of strength in the finer G branch(es) has been attributed to grain-boundary grooving, i.e. higher S due to reduced depth and increasing zigzag nature of such grooving (due to reduced G, hence more grains over a typical flaw length) with finer G, due to less severe firing to achieve finer G [13]. Thus strengths of polycrystalline ceramic fibres (which have as-fired surfaces) have been shown to be consistent with this two-branched behaviour, i.e. to typically be an extrapolation of the strength behaviour seen in bodies of normally obtained G, to the finer G typically obtained in fibres.

Where microplastic failure occurs, e.g. as can commonly be the case in dense CaO, MgO and probably $BaTiO_3$ at 22 °C, very similar behaviour is found [14]. The key difference is that the strengths of materials failing from microplastic crack nucleation (or growth),

at least at larger G, extrapolate to the stress to activate the microplastic, slip or twin system nucleating or growing the failure causing flaws (Fig. 2). Because this stress is normally only slightly below the single-crystal strength, there is no significant difference between the two. It is common for the strengths of such materials to branch to a lower G dependence of S at finer G due to failure from pre-existing flaws [14], like the finer G branches discussed earlier. (Thus, where both flaw and microplastic failure branches occur, they are opposite to what Carniglia [25] proposed; i.e. the microplastic-controlled branch is the larger, not the finer, G branch.)

2.1.3. Comparison of strength and toughness trends as a function of grain size

Comparison of the S and K trends as a function of G indicates some consistency as well as important differences. In particular, extensive S–G data (summarized above) shows the rises to K (or γ) maxima are totally unreflected in any strength data (where other variables such as P are constant, e.g. at 0, or accounted for, as is typically also the case for K and γ). This, in turn, means that bridging, to which this K rise is typically attributed, has limited, or no, impact on normal strength behaviour. One of the few exceptions to this is the SiC study of Kodama and Myoshi [31], where the strengths of their material clearly reflected the initial rising K trend with G, though the S maximum is not as pronounced as that of K. Whether these similar rises reflect some different behaviour of their polycarbosilane-derived SiC, or other factors, is not known. However, it should again be emphasized that an increasing K with G, except for the one SiC case noted above, is very inconsistent with the wealth of S–G data. It is specifically inconsistent with the S–G data for Al_2O_3 (very extensive), all BeO, all other SiC, and TiO_2, each of which has shown such K rises with increasing G [1].

There are other cases of significant discrepancies between S and K, and associated bridging. The significant K increases in Si_3N_4 as a result of developing significantly elongated (but also larger) grains are typically not reflected in strength increases, at least not at higher K, i.e. S increases less, or decreases despite K increasing two to three fold, as discussed further later (e.g. Table I). Because the K increases are attributed to accompanying bridging, this indicates that bridging has less, or no, effect on strength, at least for extensive bridging with large K increases. This is supported by the fact that the starting K before bridging occurs is approximately the same as in other materials where little or no bridging occurs. Another case of strength not reflecting the impact of bridging in $MgAl_2O_4$ made with LiF additions (and exhibiting nearly 100% intergranular fracture). The K (prior to R-curve effects) is only about 60% of the K of $MgAl_2O_4$ made without LiF (which has ~100% transgranular fracture [1, 19]). Bridging and R-curve effects are observed in the material made with LiF. However, the strengths of the material made with LiF correlates with the K not reflecting R-curve and bridging effects. The strength and K of $MgAl_2O_4$ made without LiF are higher than with LiF, but are again consistent with one another, whether K was obtained by normal fracture mechanics techniques or fractography, with no indication of bridging.

Some change in K due to the transition between polycrystalline and single-crystal K values [1, 10–16, 20] occurs in the vicinity of the finer–larger G branch intersection, but may not be necessary to account for the strength branch intersections, as discussed earlier. However, initiation of a K decrease with increasing G, e.g. as occurs with a K maximum, should correlate with such S–$G^{-1/2}$ intersections if K and related fracture energy and crack propagation tests predict strength behaviour. The locations of the K maxima [1] for Al_2O_3 (at $G \simeq 50$–100 μm), TiO_2 (at $G \simeq 15$ μm), and some Y_2O_3 data ($G \simeq 10$ μm) are not greatly inconsistent with the typical G values for the intersection of the finer and larger G branches of the corresponding typical strength–$G^{-1/2}$ plots of these materials. Further, the onset of microcracking from TEA stresses in these G ranges for Al_2O_3 and TiO_2 could be a reasonable source for both the K maxima and the greater strength decrease of the larger G branch. However, this would not explain the same basic S–$G^{-1/2}$ behaviour of cubic materials without microcracking, nor multiple finer G branches, and thus multiple finer–larger G branch intersections. An even greater S–K inconsistency is finer–larger G branches intersecting at similarly large G as for Al_2O_3, TiO_2 and $MgAl_2O_4$ not at the much finer G of the K maximum in other materials (e.g. B_4C, SiC and some Al_2O_3 and Y_2O_3) with the corresponding typical strength branches of these materials.

Attempting to correlate the K decrease from the maxima with the S decrease along the large G branch also fails. The extent of strength decrease, of course, depends on the strength level at which the finer G branch meets it, which is a function of the flaw population determining the finer G branch. S–$G^{-1/2}$ data shows such S decreases are typically about two to three fold for both cubic and non-cubic materials, but could be more because the strength minima indicated in Fig. 2 have not yet necessarily been observed. The K decrease from the Al_2O_3 maxima (associated with bridging) would provide an explanation for ~ six fold or more strength decrease (e.g. two to three times more than observed). The extent of the K decreases for TiO_2, and B_4C would be sufficient, though the latter is at far too small a G, as noted earlier. However, the strengths (of the same TiB_2 materials used in the K tests) all decrease more than the K did with increasing G [1]. More importantly, and general, is that the modest, or no, K decreases for cubic polycrystalline materials does not explain the same two to three fold observed strength decrease along their larger G branch.

More fundamentally, no decrease in the polycrystalline K is needed to explain the strength decrease along the large G branch. Thus, a polycrystalline K (or γ) independent of G, e.g as indicated for Al_2O_3 and $MgAl_2O_4$ (in the absence of bridging), or having modest decrease with G at larger G, e.g. as for Y_2O_3 and

TABLE I Weibull moduli, strength, and toughness of ceramic composites and matrices at 22 °C

material	Av. strength (MPa)	toughness ($MPa\,m^{1/2}$)	No. of tests	Weibull modulus	Reference
1. SiC[a]	600	3.2	19	16	[77]
2. Si_3N_4[a] (S, HP)	900	–	> 700	10	[78]
3. Si_3N_4 (RBSN)	300	–	30	11	[79]
4. ZrO_2 (TZP)	1100	–	30	16	[80]
5. ZrO_2 (TZP)-Sint.	1100	–	20	11	[81]
(2 mol %/Y_2O_3)-HIP	1300	10	20	14	[81]
6. SiC	400	–	–	10	[82]
7. SiC –22% TiC	500	–	9–16	12	[82]
8. Al_2O_3 –40% TiB_2	300	–	10	9	[83]
9. Al_2O_3–20% TiC[a]	600	–	15	10	Data from
	800	–	15	11	3M Co.
10. Al_2O_3[a]	440	–	24	10	
Al_2O_3–30% TiC[a]	670	–	24	5	[84]
11. Al_2O_3–SiC_w[a]	700	–	–	13	[85]
12. Al_2O_3	520	–	10	7	[86]
13. Al_2O_3–15% SiC_w[a]	680	–	10	10	[86]
14. Al_2O_3	700	–	24	6	
15. Al_2O_3–SiC_w	500	4.5–5	15	21	[87]
	770	4.5–5	20	6	[87]
	670	4.5–5	25	8	[87]
	850	4.5–5	25	6	
16.	550	11	30	18–28	[88]
17. Si_3N_4	690	8	30	19	[89]
(self-	690	8.5	15	53	[90]
18. reinforced)	600	10.3	15	25	[90]
	515	8.8	15	19	[90]

[a] The materials evaluated were commercially produced.

NiZn ferrite [1], is consistent with the S–G behaviour, because the change to single-crystal fracture toughness would typically give a factor of 2 strength decrease [1, 19, 20, 32]. The transition to grain-boundary (i.e. bicrystal) fracture toughness could decrease this by another factor of 2 or more. An important aspect of this comparison is to also consider that typically larger G strengths fall to $\sim 1/2$ or less of the average strength for the weaker orientation(s) of the corresponding single-crystal material with comparable surface finish (Fig. 2). Sufficiently low K values to reflect this decrease below single-crystal strengths are typically not observed in normal K or γ tests, if at all. However, such low strengths at large G are consistent with failure initiation along grain boundaries due to their typically lower K than for transgranular (i.e. single-crystal) fracture.

Another way to gain some insight into the applicability of polycrystalline K values to predicting strength behaviour is to compare K and E values. A correlation with K_{IC} is expected theoretically because, except for possible limited effects of Poisson's ratio, $K_{IC} = (2E\gamma)^{1/2}$. However the major theoretical determinant of γ is E, so γ correlates with E, and hence K_{IC} also does. Such E–K_{IC} correlation has previously been shown in the absence of toughening mechanisms such as transformation toughening and bridging [33–35], and is shown for the materials of this evaluation along with some other materials for reference in Fig. 3. Note that the data points scattered below the averaged trend (i.e. $MgAl_2O_4$, MgO, B, B_4C, SiC, and to a lesser extent TiO_2) all reflect extensive transgranular fracture and known, or expected, easy cleavage on one or more planes which are multiple in occurrence, e.g. {1 0 0} or {1 1 0} representing, respectively, 3 and 4 sets of planes [19]. This is in contrast to many, possibly all, of the materials above the average trend having fewer, less easy cleavage planes or both. Thus, beta alumina has only basal cleavage, i.e. only one plane, and Al_2O_3 and TiB_2 are not known to have any cleavage, and have some, to substantial, intergranular fracture [19].

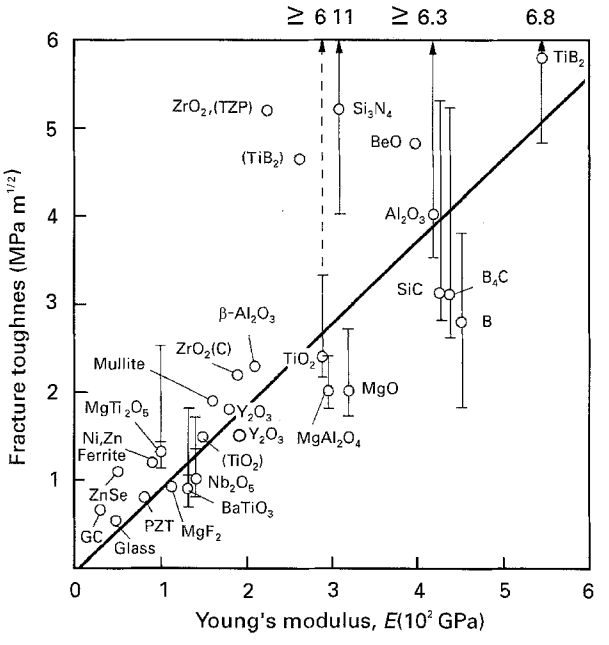

Figure 3 Fracture toughness of ceramics versus Young's modulus, E, at 22 °C.

The counterpart of the above comparison is evaluation of strength trends as a function of E. Because $S \simeq K_{IC}(C)^{-1/2}$, and polycrystalline K_{IC} values tend to be proportional to E, comparison of strengths for similar C and G values for each material should also correlate with E and give insight to S–K_{IC} relations. As the size and shape of machining flaws do not vary much for a given machining direction in test bars, many data satisfy this condition, especially at the same fine G where second-order effects on flaw geometry are not a factor. Evaluation at fine G (~ 4 μm in Fig. 4) is also important to ensure that the polycrystalline K is pertinent, rather than some value between it and single-crystal or bicrystal values. Such S–E correlation is clearly better than the K–E (Fig. 3). The three low, but not extreme, deviants from this trend, $CaZrO_3$, BeO, and TiB_2, probably reflect less development relative to most of the other materials. The extreme high deviant is tetragonal ZrO_2 (TZP), which is consistent with transformation toughening increasing K well above levels expected from those correlating with E (Fig. 3). The next highest deviant from the S–E trend is Si_3N_4, which is consistent with the lower, but not the upper, portion of its K–E trend. Similarly, note that the S–E trends do not correlate with the higher K values for TiO_2, BeO, Al_2O_3, and TiB_2. Similar issues of basic differences between S and K results will be shown for particulate composites, and even more serious differences will be shown as a function of porosity in the following sections.

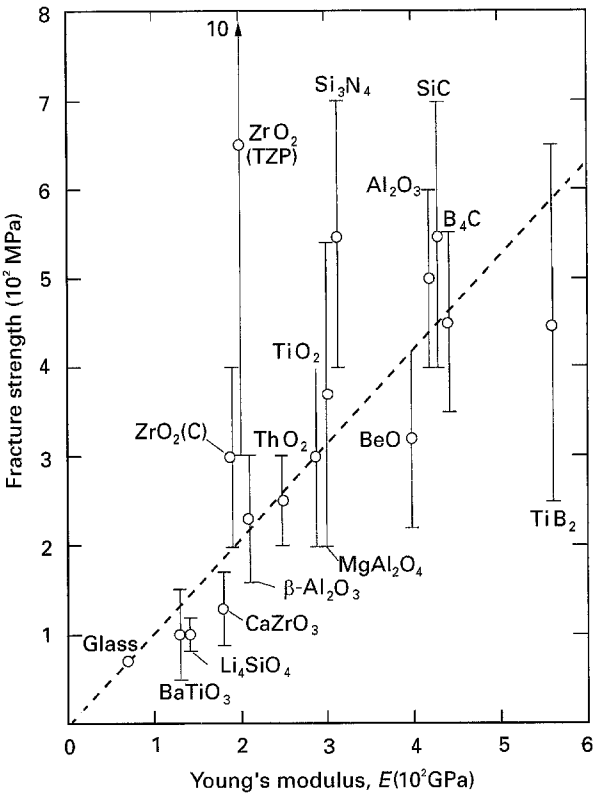

Figure 4 Strength of ceramics versus Young's modulus, E, at 22 °C.

2.2. Comparison of the effects of porosity on strength and toughness of ceramics

The effects of porosity on the mechanical properties of ceramics, though not receiving much attention, are very important in an overall understanding of their mechanical behaviour. Because the volume fraction porosity, P, effects on γ, K, and S have recently been reviewed elsewhere [1, 17, 18], they are only summarized here. The greater sensitivity, and hence the need to consider separately, the P dependence of γ stems from the fact that E has substantial dependence on P, and γ often less. Thus, the P dependence of K reflects substantial effects of E increasing its P dependence in contrast to E reducing the K dependence on grain (or particle) size relative to that of γ in previous sections.

Porosity dependence is particularly pertinent to this paper because strength and toughness show some common P trends, but also some important differences [1]. These include some cases of γ being independent of P, or possibly having some temporary increase with increasing P (e.g. $\sim 10\%$–15%). More extreme are some data for Al_2O_3 and MgO showing toughness, definitely not decreasing until $P \simeq$ 15%–25%, and possibly having a maximum at $P \simeq 10\%$–15%. At higher P cases of temporary, but significant, arrest, or temporary reversal, of the normal K, and especially γ, decrease with increasing P were found (for B_4C and RSSN, respectively). However, none of these γ or K deviations was found to correspond to the strength dependence on P, which typically followed that of E. The discrepancy between γ and K versus S was specifically seen in the case of the RSSN deviation to be due to crack branching and bridging on a scale far larger than that controlling normal strength, and hence not applicable to it [36].

Besides the above specific γ–P or K–P deviations from the S–P trends, there are much broader differences that suggest the above deviations are much more common. Strength shows a continuous decrease with increasing P that is initially approximately linear on a semilogrithmic plot of strength versus P, but then progressively decreases more rapidly to then fall precipitously to zero as the porosity at the solid percolation limit, P_c, for the particular porosity is reached. Collectively, the slope of the initial approximately linear portion (which is often expressed as the b value in e^{-bp}, which is a reasonable fit to this region of behaviour) and the $\sim P$ of both the more rapid decrease of S and the P_c characterize the porosity dependence. Such P dependence is consistent with that of most other mechanical properties, in particular E, and with predictions of minimum solid area models [16–18]. Such models predict b values of 3–5 for most pore structures, which are borne out in an extensive survey of the P dependence of strength and E (as well as of thermal and electrical conductivity) [16–18]. Of the above characteristics, the slope of the approximately linear semilogrithmic porosity dependence from $P = 0$ up to 1/3–1/2 of P_c is the most unique to a given porosity, and is most pertinent to most of the cases of interest, and is hence of central interest here.

The reduced γ and K decrease with P reduces their consistency with the minimum solid area models and frequently makes their P dependence less than that of

S and E [1]. Thus, K often also shows a similar approximately linear slope on semilog plots versus P, but with lower slopes; i.e. b values of ~ 2 versus ~ 3–4 for S and E of the same or similarly processed materials. A key exception to the above disparities is when the γ– or K–P dependence is obtained from fractography, where it is similar to that of S and E. Such consistency is expected from the Griffith equation, so long as the porosity does not significantly effect the flaw size, which it usually does not because pore sizes are usually $\ll C$, especially for substantial P [37]. The disparities in the P dependence of γ and K versus S and E, though most extensively observed for, are not restricted to, the normal P range (e.g. $< 50\%$), but also occur at high P, e.g. in foam-type materials [17].

Bridging and branching effects were indicated with large cracks in some, but not other, porous bodies. Where this occurred, it had much less, or no, effect for small cracks controlling strength, as noted above for the RSSN. This would explain the common deviations of γ and K to less P dependence than S and E. A possible basic mechanism for such bridging in porous materials is seen in cracks attempting to satisfy two, not necessarily fully compatible, criteria: fracturing through regions of the least solid area, and normal to the stress axis [17]. Heterogeneities of the porosity, in terms of size, shape and spatial distributions, are probably also major factors in the expected bridging. The variability in such effects is attributed to poorly understood crack pore–test interactions that should be a fruitful area for research.

Bridging is also probably a major reason for the significant improvement in resistance to severe thermal shock damage in many porous materials, e.g., porous refractories [10]. Thermal shock resistance is typically proportional to S or K divided by the product of E and the thermal expansion coefficient. Thus, the similar, or identical, P-dependence of E and S leave totally unexplained the large improvements in thermal shock resistance commonly resulting from porosity. This disparity is increased in the many cases in which thermal shock resistance is also proportional to thermal conductivity, which decreases with increasing P. However, because thermal shock of quite porous bodies is likely to involve propagation and arrest of larger cracks, the bridging and branching noted above with large cracks in porous bodies and resultant increases in the K/E ratio could well explain their highly improved thermal shock resistance. However, thermal stresses are usually biaxial, thus requiring study of multiaxial stresses on bridging, as noted later. Thus studies of crack bridging and branching of porous bodies should be a fruitful area for study.

It should be noted that there are coupled effects of both G and P that also lead to significant γ and K discrepancies with S [1]. Thus, in MgO, γ and K have been shown to have similar values with P a few per cent or less, as with $P = 0$, but to increase ~ 2 and 3–4 fold, respectively, as P decreased with increasing G, and shifting from mainly intergranular, to mixed inter- and intra-granular [1]. However, S does not show such effects. Similar increases in the K of sintered alpha SiC were noted, with less or no effect on S, and such P–K effects were suggested as the cause of some K–G maxima, e.g. in hot-pressed B_4C (with a few per cent P). It is clear that a body with some intragranular porosity will often reflect less P effect on S because both inter- and intra-granular porosity usually cannot be fully involved in fracture, especially if fracture is mainly inter- or mainly trans-granular. Clearly the normal large crack fracture mechanics tests cannot address such effects by themselves.

Evaluation of porosity data for Si_3N_4 indicates some toughening and strengthening due to grain-boundary phases. Thus, extrapolation of RSSN K–P data to $P = 0$ gives $K \simeq 3.5$ MPa m$^{-1/2}$ instead of the normal 4–5 + MPa m$^{-1/2}$ measured in (fine grain) dense Si_3N_4. Because the former has no grain-boundary phase and the latter does, this implies some toughening due to (oxide) boundary phases [36]. Similarly, lower extrapolation of strengths of RSSN to $P = 0$ relative to those obtained in dense Si_3N_4 made with additives implies both toughening and strengthening due to the boundary phases (and common resulting elongation of generally fine grains). As discussed later, this is consistent with crack sizes (e.g. of a few tens of micrometres) versus typical grain sizes of a few, e.g. 1–3, micrometres.

2.3 Comparison of strength and K_{IC} as a function of amount and dispersed phase size for ceramic particulate, platelet, whisker, and fibre composites

The K of composites reflects effects of the volume fraction of dispersed phase on both E and γ so, in principle, both should be considered. However, most of the composites of interest have very similar E values for both the matrix and the dispersed phase, so the variation of E with composition is much less than γ. Further the interest is greatest in the differing dependence of S and K as a function of dispersed particle size, which, as for the G dependence of the previous section, does not effect E unless it causes microcracking (which becomes important when it occurs). Thus, as with G dependence of properties, only the dispersed-phase dependence of K is considered, and not that of γ.

The K and strength dependence at 22 °C on the amount and particle size of the dispersed phase in ceramic particulate and whisker composites has been previously reviewed [6], so only key points pertinent to this paper are summarized here. Almost all particulate composites show K trends inconsistent with strength trends, e.g. Fig. 5. There Lange's K (DCB) data for Si_3N_4 with dispersed SiC particles of differing amounts and sizes clearly shows fundamentally different trends from those of strength [38], whether or not correction is made for the limited amount of porosity in some bodies. Data of Tanaka *et al.* on the same system, but with finer SiC particle sizes (and use of IF for K) [39], is a very logical extension of Lange's data. This further accentuates the differences between K and S, i.e. their going in opposite directions with the amount and size of the dispersed SiC particles. Increasing toughness with increasing particle size is

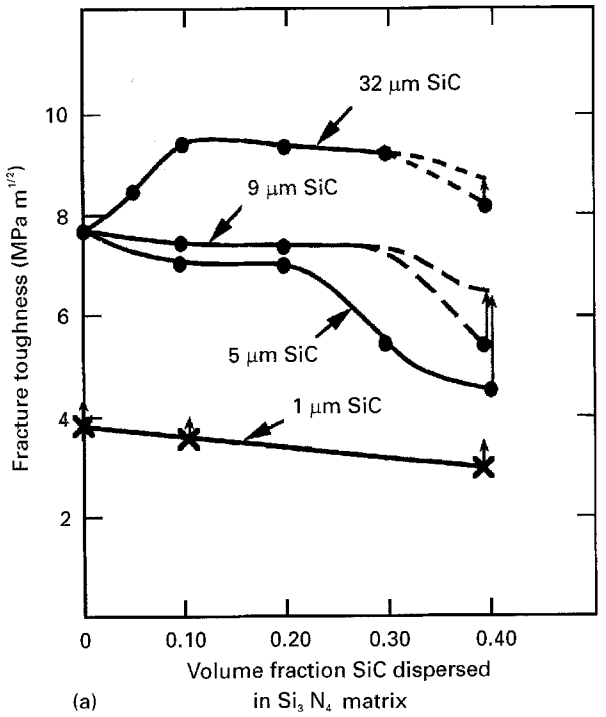

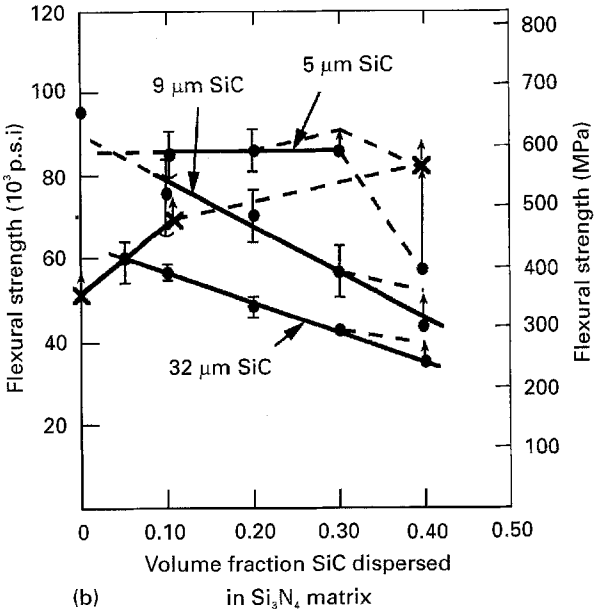

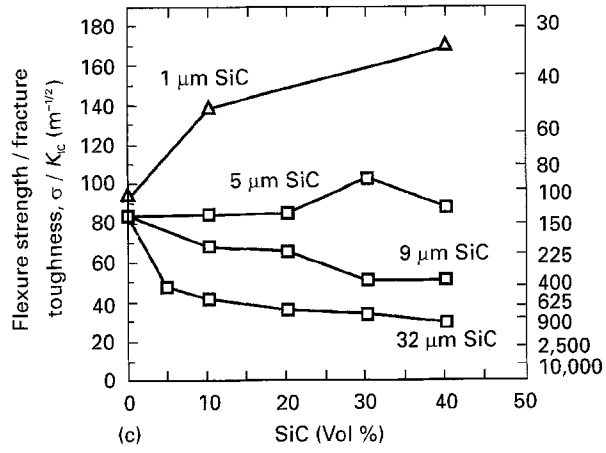

Figure 5 Strength and toughness of Si_3N_4–SiC particulate composite at 22 °C. (a) Toughness versus volume fraction SiC for various particle sizes, (b) corresponding plot of the strengths of the same specimens, and (c) corresponding plot of the strength/toughness from (a) and (b). Note corrections for limited porosity in (a) and (b), and the consistency of (●) Lange's [38] and (×) Tanaka *et al*'s [39] data in all three plots. (a, b) (●) Hot-pressed, $P \simeq 0.5\%$ to $> 5\%$; (×) sintered hot isostatically pressed, $P \simeq 3 + \%$; ↑ Porosity corrected, $b = 3$. (c) (□) Si_3N_4, Large [75], (△) Si_3N_4, Tanaka *et al.* [86].

consistent with toughening in such composites being attributed to bridging (because bridging generally increases with grain or particle size), but again shows little or no effect on strength. The S–K disparity is also shown by considering the S/K ratio, which is $\sim(C)^{-1/2}$. As shown in Fig. 5c, reasonable flaw sizes are indicated for the 1 μm, and possibly the 5 μm SiC particle bodies with typical K values, but those for the rest are grossly large. The implied flaw sizes seem far too large to reflect just processing defects. Instead, these large calculated flaw sizes probably reflect use of a K that is much greater than that controlling S, i.e. again implying that toughening effects measured by most K tests used do not necessarily reflect strength behaviour in many composites. The lower strengths of composites with larger particles are, instead, consistent with failure from one, or a few clustered, particles of the dispersed phase, and a lower K, e.g. similar to a bicrystal value in a non-composite ceramic. This is supported by the consistent decrease in S with increasing SiC particle size seen not only within studies of Lange [38], as well as within those of Nakamura *et al.* [40] and Pezzotti and Nishida [41], but also between these and other studies (Fig. 6) [39, 42, 43].

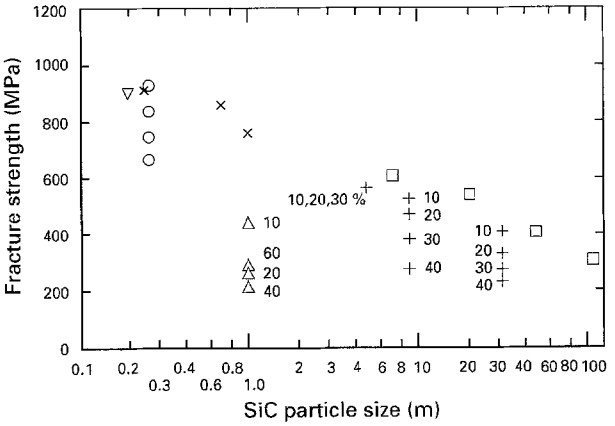

Figure 6 Strength of Si_3N_4–SiC_p composites at 22 °C as a function of SiC particle size [38–43]. (×) Nakamura *et al.* [40] 50% SiC, (□) Pezzotti and Nishida [41] 25% SiC, (+) Large [38] 10%–40% SiC, (△) Tanaka *et al.* [39] 10%–60% SiC, (○) Akimune *et al.* [42] 10% SiC, (▽) Sasaki *et al.* [43] 10% SiC.

The above results for Si_3N_4 with SiC particles are representative of other surveyed ceramic particulate composites, as well as those published since the survey. Thus, previously surveyed Si_3N_4–SiC, SiC–TiC,

SiC–TiB_2, Al_2O_3–SiC, and Al_2O_3–TiC all showed the same trends, namely strength increasing, but toughness decreasing, with decreasing dispersed particle size [6]. Again, S/K ratios indicated flaw sizes in bodies of higher K far beyond those expected from processing problems, thus indicating use of K values not reflective of those controlling strength. More recent studies generally show similar trends. Thus, Endo *et al.* [44] have shown strength of SiC increasing by about 20% as K increased by 300% (NB from a low value of $\sim 1.7\ MPa\,m^{1/2}$) with the addition of 30–60% fine ($\sim 0.4\ \mu m$) TiC particles. Bellosi *et al.* [45] also showed that addition of coarser (to $\sim 7\ \mu m$) TiN particles to Si_3N_4 increased K by $\sim 60\%$, but decreased S by $\sim 40\%$ while use of finer ($< 3\ \mu m$) TiN increased K by $\sim 100\%$ and strength by up to $\sim 20\%$. They also showed failure initiating from TiN agglomerates of up to 100 μm, or more, in size. This is consistent with results of Mah *et al.* [46] on Si_3N_4–TiC composites. They showed that addition of TiC particles (average size $\sim 8\ \mu m$, maximum $\sim 30\ \mu m$) resulted in a continuous S decrease from 700 MPa for pure Si_3N_4 until becoming constant at 450 MPa from 50–100% TiC. However, K started at $\sim 5\ MPa\,m^{1/2}$, increased to a maximum of $7\ MPa\,m^{1/2}$ at 20 vol% TiC, then decreased to a constant level of $\sim 4.2\ MPa\,m^{1/2}$, for 50–100% TiC. The decrease in S is attributed to the larger (often agglomerated) TiC particles. Such failure from microstructural heterogeneities is consistent with fracture initiation from: (1) larger Al_2O_3 grains in Al_2O_3–TiB_2 and from residual graphite particles in Al_2O_3–TiC composites (made by reaction processing) [47], and (2) foreign inclusions in many ceramics [48–50]. The only exceptions to the above trends in the previous survey and since then have been with small dispersed particles. Thus, Al_2O_3–ZrO_2 composites do show similar S and K trends with the volume fraction of fine (e.g. $< 2\ \mu m$) ZrO_2 particles, as do most other composites with fine microstructures relative to strength-controlling cracks. Crack bridging and associated R-curve effects have also now been clearly shown in many of these composites [51–53] thus explaining their high Ks.

A review of the ceramic platelet composites literature shows the same type of results as particulate composites discussed above, namely K increasing and S decreasing unless the platelets are sufficiently fine. Thus addition of 5–40 vol% Al_2O_3 platelets (e.g. 10 μm diameter) to tetragonal ZrO_2 (TZP) matrices increased K by ~ 15–60%, but reduced strengths by 20–50% [54], (and orientation of the platelets randomly, parallel, or perpendicular to the stress axis had little effect [55]). Baril *et al.* [56] also showed that uniform addition of up to 30% SiC platelets (11–24 μm diameter) to Si_3N_4 increased K $\sim 40\%$ but left S unchanged or reduced by up to 20%, while the Weibull modules was increased by up to 130%. Strength retention was distinctly best with the finest platelets. Weibull modulus results were mixed, while K results were generally independent of platelet size. Chou and Green [57] increased the K of alumina by $\sim 70\%$, but strength decreased by $\sim 30\%$ with the addition of 30% SiC platelets (12 μm diameter). Nischik *et al.* [58] did report some possible limited strength increases in mullite by addition of 10% SiC platelets (10–25 μm maximum diameter). However, strength more commonly decreased. Hanninen *et al.* [59] reported greater K increases, respectively, with larger versus smaller platelets and particulates (of similar diameter as the small platelets), but with corresponding greater S decreases as the volume fraction of particles or platelets increased. These trends are also corroborated by similar K and S trends with platelet dimensions in Al_2O_3-based composites where the platelets were produced by *in situ* reactions [60–62]. Claar *et al.* [63] reported high strengths (450–900 MPa), K values (11–$23\ MPa\,m^{1/2}$), and Weibull moduli (21–68) for ZrC matrices with in situ formed ZrB_2 "platelets". However, much, possibly all, of the improvement in mechanical properties is due to the residual zirconium content, i.e. properties increased with increased free zirconium content. Also, the "platelets" were not discs, as in most of the previous cases above, but were much closer to thicker whiskers (typically several micrometres in thickness).

Consider next whisker composites, where there are some similarities, but more differences with the trends for particulate and platelet composites. The contrasts with the latter composites is greatest for Al_2O_3–SiC_w whisker composites which were the first to be developed, and have received the most attention. Such composites that are well processed generally show S and K with similar increases with increasing whisker contents up to about 30% whiskers, where obtaining uniform bodies becomes much more difficult [64–66]. This similarity in S and K trends is in marked contrast to the opposite trends commonly found for particulate and platelet composites. In further contrasts to the latter composites, Al_2O_3–SiC_w composites show increases in K and S with increasing SiC whisker size [67, 68]. All of these trends are generally consistent with the dependences that are expected from bridging, which has been shown to occur in these whisker composites [69, 70].

Other whisker composites generally show similar K increases with increasing whisker content similar to that for the Al_2O_3–SiC_w composites, but with S commonly decreasing, as with particulate and platelet composites [6]. Some, possibly all, of this probably reflects processing problems that are well known in whisker composites. Agglomerates of whiskers and matrix grains increase in frequency and size as whisker content increases, causing strengths to not increase as much as, or to decrease, as K increases. However, it must be asked whether this is the universal reason for strength deviations in many of these composites. Si_3N_4–SiC_w which have received substantial development continue to show strength increases seriously lagging those of K, and more commonly decreasing with increasing whisker contents [71]. Thus effects of other variables need to be considered, especially the effects of whisker–matrix property differences, e.g. of thermal expansion (SiC whiskers have a lower expansion than Al_2O_3, but higher than Si_3N_4).

Finally, briefly recall the key aspects of strength and toughness of continuous fibre composites for later

discussion. These show large increases in toughness (e.g. to 30 MPa $m^{1/2}$ or more) both in actual measurements as well as in their non-catastrophic fracture with extensive fibre pullout (which is a manifestation of fibre bridging of cracks, which is well established as the major toughening mechanism in such composites). While S cannot be directly numerically correlated with K in such composites, S generally qualitatively follows K [72–74].

3. General discussion

3.1. General requirements and reliability

Four key, sometimes coupled, factors need to be addressed to begin to sort out the discrepancies between strength and fracture toughness or energy. The first is the fact that while strength is generally a necessary condition for the application of ceramics (or any brittle material) involving any significant stress, it is not sufficient; a suitably high level of reliability is also essential. Second, testing and evaluation must be sufficiently representative of the conditions that will govern fracture and failure of interest. Third, the evaluation of mechanisms controlling strength, fracture toughness/energy, and fracture should result in a rational, self-consistent view of these and related properties and behaviour, e.g. E and fracture character. Fourth is that the same toughening mechanisms, in particular those having R-curve behaviour may eliminate, or complicate the applicability of linear elastic fracture mechanics, i.e. that strength changes may not be directly, if at all, reflected by toughness changes, as is the case in continuous fibre ceramic composites. However, such S–K discrepancies should follow some rational pattern, e.g. as a function of the type, or extent of toughening.

Consider first the issue of reliability. An underlying assumption in much of the more recent study and development of ceramics, especially of ceramic composites and R-curve behaviour, has been that improving fracture toughness will improve reliability, i.e. increase the Weibull modulus, m. This, combined with the view that much of the toughening increases would not necessarily be directly paralleled by corresponding strength increases, meant less attention to strength, including commonly not measuring it. The potential for R-curve effects increasing reliability was cited by Bennison and Lawn [75], as well as Shetty and Wang [76] based on analytical evaluations. It has also been argued that wake effects are more theoretically sound and give larger K increases than crack tip toughening mechanisms [2, 3]. However, it was also shown that the impact of R-curve effects in such analyses was quite sensitive to the mathematical form used for the R-curve itself [76]. More basically, Kendall *et al.* [5] have recently presented analysis showing that an increase in toughness itself will not increase m. Also, Kovar and Readey [7] have recently shown experimentally that increasing R-curve effects in Al_2O_3 did not increase reliability, and presented arguments why this might arise from variable R-curve effects. However, they did not address the possibility that bridging was not a factor in the normal S behaviour of their Al_2O_3. In particular, they did not explain why normal (i.e. unindented) strengths of larger G Al_2O_3 were often lower than those of indented specimens. This may have resulted from failure initiating from larger grains in the unindented specimens with little, or no, contribution of bridging to S. On the other hand, the cracks from indentation may have been large enough so some bridging contribution to S occurred, increasing S over unindented values. Thus, experimentally, there are very serious questions whether the observations of bridging are relevant to most strength-controlling cracks, and whether the resultant mechanical behaviour is consistent with the effects attributed to bridging, as outlined above, and further below.

An earlier review [6] of ceramic particulate and whisker composite data showed that while toughness was often increased substantially in such composites, the Weibull moduli were not obviously increased over monolithic ceramics (commonly the matrices for the composites, Table I) [77–90]. The generally modest level of m values for ceramic composites shown in Table I is corroborated by calculations of m from coefficients of variation [91] (in composite studies where m was not measured), i.e. giving m values of 5–15. Since the earlier review, a few cases have been found that do show substantial Weibull modulus increases with toughness, but not with corresponding S increases, in fact commonly with some S limitations for *in situ* toughened Si_3N_4 [87–89].

A particularly clear case of such m increases with S limitations is Hirosaki *et al*'s study of *in situ* toughened Si_3N_4 (Table I) [90]. Their impressive Weibull modulus of 53 for their small strength specimens with fine elongated grains and (SEPB) fracture toughness of 8.5 MPa $m^{1/2}$ decreased to 25 then 19 as K first increased to 10.3 MPa $m^{1/2}$ then decreased to 8.8 MPa $m^{1/2}$, as S continuously decreased with progressive growth of elongated Si_3N_4 grains. The intermediate increase in toughness was attributed to increased bridging, and its subsequent decrease with the largest grains to microcracking from the larger elongated grains, and clusters of these. The continuous decrease in strength and Weibull modulus with increasing size of the elongated grains was attributed to first the elongated grains acting as fracture origins then clusters of them acting as origins of failure. This is supported by results of Salem *et al.* [88] showing fracture origins in their *in situ* toughened Si_3N_4 similar to those in more typical Si_3N_4, i.e. pores, pore clusters, and large grains, internally, or at the surface. These more recent studies are consistent with earlier work, e.g. of Himsolt and Kleinlein [92]. They showed both strength and toughness initially increasing with grain size and elongation (accompanying increasing α to β conversion), but strength reaching a maximum sooner than did toughness.

That microstructural sources of failure can increase the Weibull modulus in ceramics is shown by results of Biswas and Fulrath [93]. They showed that the introduction of porosity, including large (e.g. 100 μm diameter) spherical pores from burn out of latex spheres, into otherwise fully dense niobium-doped PZT, increased the Weibull modulus from 11 to 14. Failure

initiated from larger pores, or clusters of them, with the separation of such larger pores or their clusters being far too great to have produced any crack-bridging effects on S [94], which commonly decreased by $\sim 40\%$. However, the increase in m from microstructural flaws can be quite variable, e.g. calculation for the Si_3N_4–TiN composites of Bellosi *et al.* [45] give $m = 9 \pm 4$ and 22 ± 15, respectively, for their coarse and fine TiN particle additions because clusters of TiN particles were typical failure origins. The decrease in S with increasing size of the dispersed phase particles, etc., clearly correlates with the substantial fractography results noted above, earlier, and below. This is not surprising in view of larger grains, or foreign particles being common sources of failure, hence also of strength limitation [6, 46–48] in ceramics.

A key question is whether (1) the increase in m is a direct result, i.e. a consequence, of the increased toughness and related R-curve behaviour, as widely assumed, or (2) that both the K and m increases are simply parallel results of differing effects of the dispersed phase. Thus, while the dispersed phase provides toughening at large crack sizes, it may also provide a more uniform population of failure sources that would otherwise be present. This, previously raised [4], but unaddressed, possibility is clearly consistent with the reviewed results. Thus, if the increase in m was due to increased K, why is m not increased in many other cases of increased K, and where m and K both increase, why does S decrease? On the other hand, these results are consistent with m being increased due to a more uniform population of microstructural sources of failure. However, while the introduction of microstructural sources of failure appears to be a promising route to improved ceramic reliability, it requires careful development for optimum results and typically has distinct strength limitations which must be better assessed. This mechanism is, therefore, unlikely to be properly evaluated and utilized unless it is explicitly recognized, as opposed to being treated strictly as an adjunct to bridging. It also depends critically on fractography (which has been used only occasionally) for evaluation and development.

3.2. Consistency of testing and evaluation

Turning next to the need to have testing and evaluation consistent with the fracture and failure of interest, poses as serious problems as the assumption that reliability would be directly improved by increased toughness. A fundamental need is to have the microstructural effects on the failure of interest, adequately reflected in tests and analysis to understand or predict such failure. This basic requirement is often violated where failure occurs from much less than a statistical sampling of the microstructural features that significantly impact the failure of interest. Thus, most crack propagation, i.e. including most K and γ, tests use cracks whose length, extent of propagation, or both are large in comparison to the pertinent microstructural features. Thus, when failure initiates from only part of a grain in a uniform, or a heterogenous microstructure, tests not reflecting effects of microstructural stresses [21, 22] or the transition to single or bicrystal Ks or their equivalents in composites, are not valid for such failure. Similarly, tests that reflect effects of pores that are not associated with strength failures are misleading. Modification of the tests and use of fractography are key needs [26].

Even more basic and general questions arise concerning bridging and R-curve observations. While there has been some attention to smaller cracks [22], most cracks used are still large in comparison to key microstructural features. Almost all bridging observations are made, in vacuum (in a SEM), at the intersection with a free surface, of a large crack under uniaxial stress that has travelled mostly at low (generally uncertain) velocities, then commonly arrested, often repeatedly. This is fundamentally different from most failure, where (1) much of the critical crack propagation for a surface crack, and all of that of an internal crack not near the surface, must occur in the sample, not along its intersection with the surface, (2) cracks are much smaller, and often do not represent a statistical sampling of the microstructural features controlling mechanical properties, (3) crack propagation is often effected by the environment, e.g. H_2O, and (4) the stress may not be uniaxial. The extent to which bridging occurs along a crack front away from a free surface (and frequently other cracks, e.g. from machining) is, at best, poorly documented. Not only has the issue of microstructural scale not been adequately addressed, but the statistics of bridging events, e.g. average spacings between bridges as a function of microstructure, have not been presented. Much more quantitative statistical data are needed because tensile failure is a weak link process, so failure will be controlled by the region of least, not the average or most, bridging if this hinders failure. Environmental effects on bridging are also not clear, despite the fact that environmental effects on crack growth are significant in Al_2O_3, which has been the source of much of the bridging observations, and in which such crack growth is often preferentially by intergranular fracture, favouring bridging. Also, while many failures occur under uniaxial loading, many do not, so effects of more complex stresses on bridging are needed, e.g. the biaxial stress as with many thermal stresses and used in some, tests to apply bridging concepts to strength.

An extension of the crack size issue is the rate of increase of toughness due to bridging or other mechanisms as crack propagation occurs. Examination of such crack-size effects on toughness is needed at finer crack sizes and over a broader range of grain and particle sizes and porosity. Similarly the effects of crack size on fatigue, which tends to show higher crack growth in fatigue at finer crack sizes [95, 96] need investigation over a similarly expanded range of parameters. An additional, simple, but potentially very valuable test would be measurement of strengths as a function of specimen size. Specifically, measurement of strengths as the cross-sectional dimensions of the specimens decreases to, and potentially below, the ultimate crack size expected at the point where catastrophic failure occurs, could be definitive, as follows.

If the specimen dimensions fall to, or below, the crack sizes expected from bridging effects (e.g. to 1/2–1 mm), then if bridging is occurring, strengths should start to decrease as specimen sizes decrease below such crack sizes. This would thus be a reversal of, and hence in marked contrast to the normal, continued increase in the strength as specimen size decreases.

Finally, if crack-wake effects such as bridging are significant in controlling failure, then the rate of increase of crack wake area per unit area of crack should be important [96]. However, this rate depends substantially, e.g. by a factor of 2 or more, on crack geometry, raising the question of whether cracks used in tests must adequately reflect the geometry (as well as the size as noted earlier) of the cracks causing failure. (Note that for mechanisms effecting crack propagation that occur along the periphery, i.e. at the tip, of the crack, the rate of change of the peripheral length of the crack per unit of crack peripheral length is much less than for wake-area changes.) Thus, other mechanisms such as microcracking, which are shown in some studies of ceramic particulate composites [51], should not be neglected.

3.3. Consistency of mechanisms of various ceramics and composites

Consider next the issue of self consistency amongst the different types of composites. Continuous fibre composites that are very tough clearly have extensive R-curve behaviour and fibre bridging and resultant fibre pullout which is the major source of toughness. Because of the extensive bridging, high toughness, and matrix microcracking in these composites, failure cracks are large in comparison with the composite microstructure and propagate stably, generally with repeated deceleration and acceleration, not catastrophically, so there is no specific failure origin. Therefore, bridging observations are consistent with such composite failures and the character of cracks involved, including the resultant fracture character. Thus, not only is fibre bridging observed across the fractures, the extent of this basically (though not necessarily directly quantatively) correlates with the toughness, and is corroborated by the occurrence of other fracture features, e.g. the occurrence of high-strength fracture mirrors on pulled-out fibres, and the absence of these when no fibre pullout occurs [72, 73].

Whisker composites, which are the next most similar to fibre composites, exhibit some similarities and some important differences in behaviour from fibre composites. The similarities are in the fibrous nature of the whiskers, the occurrence of R-curve behaviour and some bridging in crack propagation tests. The substantial mixture of "intergranular" and "transgranular" fracture of whiskers on fractures from slow and fast cracks is consistent with some whisker bridging of cracks, but grossly less than in fibre composites. (The generally substantial transgranular fracture of the matrix grains, e.g. Al_2O_3, is not inconsistent with fibre composite fractures, nor necessarily with whisker bridging.) The limited data on increasing S and K with increasing whisker diameter are consistent with bridging predictions. The major differences from fibre composites in terms of microstructure are the geometry, especially length and orientation, as well as the volume fraction of the whiskers, and probably their bonding to the matrix. The properties and behaviour of whisker composites contrast to fibre composites in two key ways. The first is catastrophic failure and related phenomena such as apparently general (and frequently confirmed) failure initiation from a specific source (such as clusters of, or larger, matrix grains, or of whiskers, and possibly larger whiskers) [6, 86, 98], with some quantative correlation of such origins and (lower) measured K values [86, 98]. At least some of the characteristic catastrophic fracture features such as crack branching should also occur, but little, or no, observation or study has been made of this. Second, is the generally reasonable correspondence between S and K, at least in some systems, especially Al_2O_3 –SiC_w, until high whisker loadings, where heterogeneities begin to dominate. Other systems generally do not show nearly as much, if any S–K correspondence.

Platelet composites contrast to whisker composites in both geometry and mechanical behaviour. While they show some bridging and R-curve behaviour, this appears to be less than in whisker composites, which is consistent with considerably less surface area (and equal or greater bonding to the matrix than whiskers, hence generally less "intergranular" platelet fracture.). A key difference is that platelet composites almost, if not always, show opposite S and K trends with platelet composite parameters such as volume fraction, platelet dimensions and orientation. This cannot be attributed primarily to heterogeneities from processing because platelet composites are less susceptible to such heterogeneities than whisker composites, e.g. due to the lower surface area for the same volume fraction of platelets and whiskers. It seems unlikely that this opposite trend of K and S can be attributed to toughening no longer being a direct predictor of strength, for two reasons. First, the toughness of platelet composites is generally not significantly more, and commonly less than for whisker composites (consistent with less bridging and pullout), while whisker composites show more reasonable K–S correlations. Second, the much greater lateral dimensions and frequently greater thickness of platelets all provide greater opportunity for them, especially with some clustering (as frequently observed) to act as fracture origins, but little, or no, detailed examination of this has been made. Much finer platelets may result in toughness and strength trends being closer, as for particulate composites. However, the combination of the above observations suggests that the toughening in existing platelet composites (as observed with large cracks) has limited, or no, relation to strength behaviour. Instead strengths are likely to be controlled by the more local toughness of the interfaces between larger platelets or agglomerates of them and the matrix.

Particulate composites extensively show opposite S and K trends, with strengths decreasing with increasing particulate content until dispersed particle

sizes are small, e.g. $\sim 1\ \mu m$. These trends question whether bridging and related R-curve effects determine strength over the broad (often the complete) microstructural range commonly assumed. The argument that K no longer correlates with S does not appear to be valid in these materials in view of the better correlation in whisker and fibre composites, respectively with higher, and much higher, K than particulate or platelet composites. The same argument holds for TZP materials, where the clear effects of transformation, mainly effective through their effects on the crack wake, are still consistent with fracture mechanics until quite high toughnesses are reached [99]. The substantial transgranular fracture of both the composite matrix and the dispersed phase that frequently occurs [19] also questions the role of bridging in view of it commonly being favoured by intergranular rather than transgranular fracture. The decrease in strength with increasing particle size suggests that individual or clustered particles act as fracture origins, which is confirmed in the limited fractographic examinations that have been made [6, 45]. Such initiation also questions strengths being determined by bridging and R curve phenomena, e.g. because larger particles should be associated with greater toughness and hence not an area for failure initiation.

The common absence of bridging effects on S, i.e. the frequently poor, or opposite trends of S and K, cannot be simply attributed to microstructural inhomogeneities of composites from imperfect processing. Such S–K deviations are, instead, seen as evidence for often limited, or no, bridging contributions to S for two basic reasons. First, if bridging had significant effects on S, they should still contribute to S despite some reasonable level of microstructural hetrogeniety. Second, the S–K discrepancies do not correlate with processing difficulties or level of development. Thus, processing of whisker composites presents more challenges to homogeneity than processing platelet composites, and both of these present more challenges than processing particulate composites. However, S–K deviations are typically greatest for particulate composites and least for whisker composites. Also, serious S–K differences occur for extensively manufactured composites, e.g. Al_2O_3–TiC and WC–Co [6].

The inconsistent strength and toughness trends of ceramics as a function of G or P also question bridging and R-curve effects as broadly determining strength. The consistency of fracture toughness measured with little or no R-curve effect with those calculated from fractography, and the latter showing essentially the same P dependence as S and E even more seriously question this. The frequent occurrence of failure initiation from one, or a few, larger grains raises the same issues as failure initiation from larger particles in composites. Failure initiation commonly observed from one or a few pores also raises serious questions, because a pore provides no wake area for bridging. Thus, wake-area phenomena can only occur as a crack expands away from the pore. However, failure analysis shows that failure occurs when the crack size is not much larger than the pore from which it initiated. Thus, if bridging were important to normal strength behaviour, one would expect to find lower strengths for failure from pores than most other sources due to less bridging with failure from pores. There is no evidence of this, but strong indications to the contrary.

Again fracture mode is an important issue. Most dense, and many porous ceramics exhibit predominantly transgranular fracture [19], which is less favourable to bridging. Fracture initiation from larger grains may be intergranular or transgranular, independent of the surrounding fracture mode, with no obvious S or K difference. Because bridging is more commonly associated and more effective, with intergranular fracture, why do such fractures not have higher toughness and strength? Also note again that use of LiF to densify $MgAl_2O_4$ results in reduced S and K, but increased bridging [1]. Finally, note that while the focus has been on bridging because of its potential applicability to many more materials, similar questions arise regarding the applicability of R-curve effects from transformation toughening. Only at the extremes of very high toughness or microstructure (i.e. microcracked material) do strength and toughness not correlate in the normally expected fashion, which is attributed to the transformation process itself, at the extreme increasing K, but decreasing S [97]. Otherwise, measured toughness and that calculated from fractography of flexure-tested samples agree [16, 21, 22, 32].

Overall the key to this issue of the role of bridging (and other toughening mechanisms) appears to be the scale of the cracks causing failure to the scale of the microstructural features significantly impacting their propagation up to the point of catastrophic failure. Thus, in most TZP materials, failure-causing cracks are large in comparison to the grains, and so hence are the transformation events and resultant local stresses. Therefore, strength and toughness correlate, and fracture mechanics applies. Similarly, bridging or other toughening mechanisms may increase strengths of finer grain Si_3N_4 and SiC made with oxide additives, but toughness and strength correlate and fracture mechanics is valid as normally applied. However, as coarser grain structures are developed which give clear and substantial bridging effects (with intergranular fracture), the grains, or commonly clusters of them become the sources of failure thus limiting strengths below those predicted from the large crack toughness. This occurs when such grains or clusters approach a sufficient fraction of the critical flaw size. Note that in such cases the toughness controlling the initiation of failure is that approaching, or even below, that for cleavage of a grain, or that of grain boundaries for intergranular failure. The parameters here are expected to be the number of grains involved, their character (e.g. elongation and relative orientation to each other and the developing crack) and the amount and character of the (often excessive) grain-boundary phase locally present.

3.4. Consistency with other fracture features and test conditions

Two other areas of consistency that are important to consider are other aspects of fracture and behaviour

under other test conditions. While the issue of fracture mode has been addressed above, a related issue is the impact on basic fracture features; specifically the onset of mist, hackle, and especially crack branching that surround the fracture "mirror". (Crack branching is emphasized because mist and hackle may be obscured or altered by dispersed phases.) The distances from the fracture origin to the onset of these features, divided by the flaw size is a function of the toughness controlling fracture [98]. If that toughness increases significantly as the crack progresses, i.e. being higher prior to initiation of catastrophic fracture as implied by wake concepts, then this should be discernable as an increase in these characteristic dimensions. (Unfortunately, observation of increases in these dimensions is not necessarily definitive. Increases in these dimensions would also occur if bridging occurred as the crack continues to propagate after catastrophic failure has commenced. This could readily occur if bridging can occur at terminal crack velocities because catastrophic crack propagation occurs at a modest fraction of the mirror size.) Dimensions of these features in composites has been examined very little. The limited data actually show the mist and hackle boundaries being smaller in composites, which may simply reflect their easier nucleation due to the presence of the second phases (or of non-cubic ZrO_2 in TZP) [100]. Data for the crack branching to flaw size ratio are very limited and uncertain, but do not show obvious shifts. However, there are substantial data for dense, monolithic ceramics (e.g. aluminas), which show no clear differentiation between materials associated with varying degrees of bridging.

The issue of consistency with failure under other test conditions entails both different stress, as well as different test environments which have recently been reviewed for S [15]. The issue of slow crack growth due to environmental effects, which commonly favours intergranular fracture and thus bridging, was raised earlier. Thus, slow crack growth should impact bridging, presumably enhancing it, as does the presence of residual additives at grain boundaries, in $MgAl_2O_4$. However, slow crack growth, and resultant delayed failure, occur with small cracks in dense Si_3N_4 made with oxide additives (giving mainly intergranular fracture, hence more opportunity for bridging), but not with large cracks [101], i.e. opposite to the grain-size trends expected for bridging. Slow crack growth also ties in with the broader variable of test temperature, T. Testing at lower T, e.g. $-196\,^{\circ}C$, where slow crack growth is eliminated, typically increases strength. If this reduces bridging, and hence also toughness from resultant R-curve effects, why does strength not decrease at the lower temperature if such effects impact strength?

On the other hand, as T increases a few to several hundred degrees above $22\,^{\circ}C$ strengths may increase, or decrease, a little, and in some cases substantially (e.g. ~70%) [15]. Decreases and increases may occur sequentially, and be dependent on G. Thus, most Al_2O_3 bodies show strength decreasing to a minimum at ~ 300–700 °C, then rising to a maximum at ~ 1000 °C. Recent results of White and Hay [102] showing both fracture toughness and R-curve effects in an alumina decreasing from 22–600 °C (the range tested, accompanied by modest decrease of transgranular fracture) may be consistent with such a minimum. However, this correlation is most likely coincidental because there is no basis for bridging effects being consistent with (1) a subsequent strength maximum, (2) the minimum and maximum being more pronounced for medium and larger, and of doubtful existence for finer, grain sizes, and (3) the most extreme changes occur in sapphire crystals and filaments [15].

The strength of BeO increases to G-dependent maxima at ~ 600–1000 °C that are 10%–80% greater than at 22 °C. While this might suggest bridging, the greatest changes occur at smaller to medium G, and the least at large G, i.e. not necessarily what would be expected from the G dependence of bridging, though fracture mode changes [19] could be a factor. On the other hand, MgO shows a progressively less than normal S decrease with increasing T below 1000 °C as G increases, and a modest (~ 10%) increase to a maximum at ~ 700 °C for large G, where there is more transgranular fracture. Thus, this is not likely to reflect effects of bridging, but could well reflect other factors such as increased dislocation effects [103]. In contrast to the above behaviour, polycrystalline, fully stabilized ZrO_2 shows anomalously greater strength, and somewhat greater E decreases with increasing, especially at < 700 °C, and some increase in intergranular fracture. However, these trends are opposite to what might be expected for bridging, i.e. the increased intergranular fracture would be expected to increase, not decrease the strength, and do not explain the E decrease. The latter appears to correlate with changes in lattice defects and accompanying changes in dielectric loss and internal friction [15]. Thus the changes of strength with increasing T, while in a few cases possibly being consistent with bridging, overall poses serious problems for bridging. It also reinforces the view that *various* mechanisms impact flaw failure, and hence strength, not primarily one.

Consider now effects of other stressing modes besides the simple uniaxial tensile stressing of bridging observations. Progressing from uniaxial to biaxial and triaxial stresses may well reduce bridging because the added stress components should progressively reduce the occurrence, or effects of, bridging, e.g. reducing the elastic interference of bridging grains. Despite these uncertainties, bridging concepts have been applied to biaxial fracture without any discussion of their applicability. Such issues are important because multiaxial stresses are important in practice. An important case is thermal stresses which, at the minimum have a significant biaxial character. In the case of serious thermal stresses substantial crack growth can occur, potentially making bridging observations more applicable because of the resultant larger crack size, but uncertain because of the multiaxial stress.

Another stress aspect of importance from both a practical and a scientific standpoint is that of repeated stresses, i.e. of fatigue. Fatigue tests of specimens with small (natural) flaws, moderate (indent) flaws and with larger cracks, which commonly show faster, as

well as significantly different, crack growth as flaw size decreases [95, 96]. This clearly implies less, or no, bridging effects active with smaller flaws. This greater crack growth with smaller flaws is reported for materials such as Al_2O_3–SiC_w and partially stabilized zirconias.

4. Conclusion

The substantial attention given to *R*-curve effects, especially from bridging, has been driven by the higher toughness they can give, and hoped-for resultant increases in reliability. However, two sets of observations now seriously question broad applicability of these effects. First, there is increasing evidence that such toughening does not necessarily increase reliability. There are some cases where the Weibull modulus does increase with microstructures that exhibit bridging. However, such cases appear to result from the grains or particles causing bridging also acting as a more uniform source of fracture origins. This deserves further study, because (1) it may be useful, but means more limited strengths, and (2) it cannot be properly studied or optimized unless it is explicitly recognized instead of being treated as an adjunct to bridging.

The second set of observations seriously questioning the broad applicability of bridging are those comparing strength, toughness and related properties as a function of microstructure. The observation of such bridging and *R*-curve effects have been made with large cracks. However, such effects must be shown to be applicable on the scale of the flaws controlling strengths in order to predict strengths. A review of the dependence of fracture energy and toughness, and of strengths as a function of grain size, porosity, and the amount and character of composite-dispersed phases shows limited or no correlation between *R*-curve, bridging and related large crack phenomena with normal strength behaviour for most materials. Consideration of environmental and temperature effects further questions the applicability of such large crack phenomena to strength behaviour. Thus, blanket acceptance of wake effects, especially crack bridging, as the primary determinant of toughness controlling normal *S* and the reliability of many ceramics and ceramic composites, is not justified. While the validity of these effects is clearly established in fibre composites, it varies from somewhat uncertain applicability to being most likely not applicable in many materials for many common failure conditions. A key issue commonly not adequately addressed is the scale of the cracks causing failure to those for characterizing fracture behaviour, and especially the scale of both of these to the critical microstructural features. It is also important that other reasonable toughening mechanisms, though not offering the same level of toughening, are not discarded or neglected without sufficient evidence. While some reliability increases have been observed with high toughness attributed to bridging, these appear to be the result of larger grains, or clusters of them, acting as a more uniform population of failures sources. Thus, the increased toughness and reliability appear to be parallel results of the microstructural effects rather than the toughness itself increasing the Weibull modulus. Optimization of such reliability increases, i.e. to minimize the limitations on strength indicated, will require explict consideration of a parallel, as opposed to just a cause and effect, relation between strength and toughness. Thus, much more thorough test and evaluation (including fractography) are needed on this and related studies as recommended.

Note added in proof

It has recently come to the author's attention that similar discrepancies in the microstructural trends for fracture toughness and tensile strength also occur in cements and concretes. Thus, Eden and Bailey [104] reported that removing large pores ($> 100\ \mu m$ dia.) from their Portland cement paste (by de-airing), increased strength by $\sim 15\%$, it made a similar decrease in K_{IC}, i.e. similar to some of the temporary reversals of K_{IC} decreasing with increasing porosity. R-curve effects, i.e. a temporary increase in K_{IC} with increasing crack propagation and hence length, are observed in cement pastes, and have been associated with a microcracking zone (as revealed by dye penetration examination) around the microcrack [105]. Strange and Bryant [106] showed similar, but substantially larger discrepancies for two concretes as a function of aggregate type and size. While increased aggregate size increased toughness, it decreased strength for two different aggregates. They attributed the decreased strength with increased aggregate size to aggregate pieces acting as failure initiation sites, i.e. the same as shown earlier in this paper for ceramic composites.

References

1. R. W. RICE, *J. Mater. Sci.* **31** (1996) 1969.
2. A. G. EVANS, *J. Am. Ceram. Soc.* **73** (1990) 187.
3. F. GUIU and R. N. STEVENS, *J. Mater. Sci.* **26** (1991) 4375.
4. R. W. RICE, *J. Am. Ceram. Soc.* **76** (1993) 1898.
5. K. KENDALL, N. Mc ALFORD, S. R. TAN and J. D. BIRCHALL, *J. Mater. Res.* **1** (1986) 120.
6. R. W. RICE, *Ceram. Eng. Sci. Proc.* **11** (1990) 667.
7. D. KOVAR and M. J. READEY, *J. Am. Ceram. Soc.* **77** (1994) 1928.
8. R. W. RICE and S. W. FREIMAN, in "Ceramic Microstructures '76: With Emphasis on Energy Related Applications", edited by R. M. Fulrath and J. A. Pask (Westview Press, Bolder, CO. 1977) pp. 800–23.
9. R. W. RICE, S. W. FREIMAN and P. F. BECHER, *J. Am. Ceram. Soc.* **64** (1981) 345.
10. R. W. RICE, in "Fracture Mechanics Methods for Ceramics, Rocks, and Concrete", edited by S. W. Freiman and E. R. Fuller Jr ASTM STP 745 (American Society for Testing and Materials, Philadelphia, PA, 1982) pp. 96–117.
11. *Idem*, *Proc. Br. Ceram. Soc.* **20** (1972) 205.
12. *Idem*, in "The Science of Ceramic Machining and Surface Finishing II", edited by B. J. HOCKEY and R. W. RICE NBS Special Publication 562 (US Government Printing Office, Washington DC, 1979) pp 429–54.
13. *Idem*, submitted to *J. Mater. Sci.*
14. *Idem*, submitted to *J. Mater. Sci.*
15. *Idem*, submitted to *J. Mater. Sci.*
16. *Idem*, in "Treatise on Materials Science and Technology", Vol. 11, "Properties and Microstructure", edited by R. K.

MAC CRONE (Academic Press, New York, 1977). pp 191–381.
17. *Idem, J. Mater. Sci.* **31** (1996) 102.
18. *Idem, J. Mater. Sci.* **31** (1996) 1509.
19. *Idem*, in "Fractography of Glasses and Ceramics III", Ceramic Trans., V64, edited by V. D. Fréchette and G. D. Quinn (American Ceramic Society, Westerville OH, 1996) p 1.
20. R. W. RICE, S. W. FREIMAN and J. J. MECHOLSKY JR, *J. Am. Ceram. Soc.* **63** (1980) 129.
21. R. W. RICE, R. C. POHANKA and W. J. MCDONOUGH, *ibid.* **63** (1980) 703.
22. R. F. COOK, B. R. LAWN and C. J. FAIRBANKS, *ibid.* **68** (1985) 604.
23. P. CHANTIKUL, S. J. BENNISON and B. R. LAWN, *ibid.* **73** (1990) 2419.
24. K. HAYASHI, Y. TATEWAKI, S. OZAKI and T. NISHIKAWA, *J. Ceram Soc. Jpn Int. Ed.* **96** (1988) 516.
25. S. C. CARNIGLIA, *J. Am. Cer. Soc.* **48** (1965) 580.
26. R. W. RICE, in "Fracture Mechanics of Ceramics", edited by R. C. BRADT, D. P. H. HASSELMAN and F. F. LANGE (Plenum Press, New York, 1974) pp. 323–43.
27. *Idem*, "Machining of Advanced Materials", edited by S. JOHANMIR NIST Special Publication **847** (US Government Printing Office, Washington DC, 1993) pp. 185–204.
28. J. P. SINGH, A. V. VIRKAR, D. K. SHETTY and R. S. GORGON, *J. Am. Ceram. Soc.* **62** (1979) 179.
29. A. G. EVANS, *ibid.* **63** (1980) 115.
30. A. V. VIRKAR, D. K. SHETTY and A. G. EVANS *ibid.* **64** (1981) 56.
31. H. KODAMA and T. MIYOSHI, *ibid.* **73** (1990) 3081.
32. R. W. RICE, "Ceramic Transactions", Vol. 17 "Fractography of Glasses and Ceramcis II", edited by V. D. FRECHETTE and J. R. VARNER (American Ceramic Society, Westerville, OH, 1991) pp. 509–45.
33. J. J. MECHOLSKY JR, S. W. FREIMAN and R. W. RICE, *J. Mater. Sci.* **11** (1976) 1310.
34. R. W. STEINBRECH, *J. Eur. Ceram. Soc.* **10** (1992) 131.
35. S. SAITO (ed.), "Fine Ceramics" (Elsevier, New York, 1988) p. 183.
36. R. W. RICE, K. R. McKINNEY, C. CM. WU, S. W. FREIMAN and W. J. McDONOUGH, *J. Mater. Sci.* **20** (1985) 1392.
37. R. W. RICE, *J. Am. Ceram. Soc.* **77** (1994) 2232.
38. F. F. LANGE, *ibid.* **55** (1973) 445.
39. H. TANAKA, P. GREIL and G. PETZOW, *Int. J. High Temp. Ceram.* **1** (1985) 107.
40. H. NAKAMURA, S. UMEBAYASHI and K. KISHI, in *J. Cer. Soc. Jpn Int. Ed.* **97** (1989) 1526.
41. G. PEZZOTTI and T. NISHIDA, *J. Mater. Sci.* **29** (1994) 1765.
42. Y. AKIMUNE, T. OGASAWARA and N. HIROSAKI, *J. Ceram. Soc. Jpn Int. Ed.* **100** (1992) 468.
43. G. SASAKI, H. NAKASE, K. SUGANUMA, T. FUJITA and K. NIIHARA, *ibid.* **100** (1992) 536.
44. H. ENDO, M. UEKI and H. KUBO, *J. Mater. Sci.* **26** (1991) 3767.
45. A. BELLOSI, S. GUICCIARDI and A. TAMPIERI, *J. Eur. Ceram. Soc.* **9** (1992) 83.
46. T. MAH, M. G. MENDIRATTA and H. A. LIPSITT, *Am. Ceram. Soc. Bul.* **60** (1981) 1229.
47. C. P. CAMERON, J. H. ENLOE, L. E. DOLHERT and R. W. RICE, *Ceram. Eng. Sci. Proc.* **11** (1990) 1190.
48. H. R. BAUMGARTNER and D. W. RICHERSON, in "Fracture Mechanics of Ceramics", Vol. 1, edited by R. C. BRADT, D. P. H. HASSELMAN and F. LANGE (Plenum Press, New York, 1974) pp. 307–86.
49. A. G. EVANS, *J. Mater. Sci.* **9** (1974) 1145.
50. R. W. RICE, "Processing of Crystalline Ceramics", edited by H. PALMOUR III, R. F. DAVIS, and T. M. HARE (Plenum, New York 1978) pp. 303–19.
51. W.-H. GU, K. T. FABER and R. W. STEINBRECH, *Acta Metall. Mater.* **40** (1992) 3121.
52. M. K. BANNISTER and M. V. SWAIN, *J. Mater. Sci.* **26** (1991) 6789.
53. S. V. NAIR, P. Z. Q. CAI and J. E. RITTER, *Ceram. Eng. Sci. Proc.* **13** (1992) 81.
54. K.-H. HEUSSNER and N. CLAUSSEN, *J. Eur. Ceram. Soc.* **5** (1989) 193.
55. X.-N. HUANG and P. S. NICHOLSON, *J. Amer. Cer. Soc.* **76** (1993) 1294.
56. D. BARIL, S. P. TREMBLAY and M. FISET, *J. Mater. Sci.* **28** (1993) 5486.
57. Y.-S. CHOU and D. J. GREEN, *J. Am. Ceram. Soc.* **76** (1993) 1452.
58. C. NISCHIK, M. M. SEIBOLD, N. A. TRAVITZKY and N. CLAUSSEN, *ibid.* **74** (1991) 2464.
59. M. HANNINEN, R. A. HABER and D. E. NIESZ, in "Ceramic Transactions", Vol. 19, "Advanced Composite Materials", edited by M. D. SACS (American Ceramic Society, Westerville, OH, 1991) pp. 749–55.
60. T. KOYAMA, A. NISHIYAMA and K. NIIHARA, *J. Mater. Sci.* **29** (1994) 3949.
61. H.-D. KIM, I.-S. LEE, S.-W. KANG and J.-W. KO, *ibid.* **29** (1994) 4119.
62. Y. K. BAEK and C. H. KIM, *ibid.* **24** (1989) 1589.
63. T. D. CLAAR, W. B. JOHNSON, C. A. ANDERSON and G. H. SCHIROKY, *Ceram. Eng. Sci. Proc.* **10** (1989) 599.
64. T. N. TIEGS and P. F. BECHER, *ibid.* **7** (1986) 1182.
65. P. F. BECHER, C.-H. HSUEH, P. ANGELINI and T. N. TIEGS, *J. Am. Ceram. Soc.* **71** (1988) 1050.
66. P. F. BECHER, H. T. LIN and K. B. ALEXANDER, in "Science of Engineering Ceramics'91", edited by S. KIMURA and K. NIIHARA (Ceramic Society of Japan, 1991) pp. 307–14.
67. B. J. WRONA, J. F. RHODES and W. M. ROGERS, *Ceram. Eng. Sci. Proc.* **13** (1992) 653.
68. J. RODEL, E. R. FULLER JR and B. R. LAWN *J. Am. Ceram. Soc.* **72** (1991) 3154.
69. P. F. BECHER, E. R. FULLER JR and P. ANGELINI, *ibid.* **74** (1991) 2131.
70. S. IIO, M. WATANABE, M. MATSUBARA and Y. MATSUO *ibid.* **72** (1989) 1880.
71. J. HOMENY and L. J. NEERGAARD, *ibid.* **73** (1990) 3493.
72. R. W. RICE and D. LEWIS III, in "Ceramic Fiber Composite Based Upon Refractory Polycrystalline Ceramic Matrices", Reference Book for Composities Technology, edited by S. M. LEE (Technomic, Lancaster, PA, 1989). pp 117–42.
73. R. W. RICE, J. R. SPANN, D. LEWIS and W. COBLENZ *Ceram. Eng. Sci. Proc.* **5** (1984) 614.
74. J. F. JAMET, D. LEWIS and E. Y. LUH, *ibid.* **5** (1984) 625.
75. S. J. BENNISON and B. R. LAWN, *Acta. Metall.* **37** (1989) 2059.
76. D. K. SHETTY and JR-S. WANG, *J. Am. Ceram. Soc.* **72** (1989) 1158.
77. Y. HAMANO, M. YAMAGUCHI and S. NAGANO, in "Ceramics for High Performance Applications, III Reliability", edited by E. M. LENOE, R. N. KATZ and J. J. BURKE (Plenum Press, New York, 1983) pp. 251–66.
78. E. M. LENOE, *ibid.*, pp. 3–18.
79. E. A. FISHER and W. TRELA, *ibid.*, pp. 623–43.
80. J. SUNG and P. S. NICHOLSON, *J. Am. Ceram. Soc.* **71** (1988) 788.
81. K. TSUKUMA and M. SHIMADA, *Am. Ceram. Soc. Bull.* **64** (1985) 310.
82. M. A. JANNEY, *ibid.* **66** (1987) 322.
83. W. STADLBAUER, W. KLADNIG and G. GRITZNER, *J. Mater. Sci. Lett.* **8** (1989) 1217.
84. M. WATANABE and I. FUKUURA, "The strength of Al_2O_3 and Al_2O_3-TiC Ceramics in Relation to Their Fracture Sources", Ceramic Science and Technology at the Present and in the Future, Japan, (1981) pp. 193–201.
85. E. D. WHITNEY, *Am. Ceram. Soc. Bull.* **67** (1988) 1010.
86. R. K. GOVILA, *J. Mater. Sci.* **23** (1988) 3782.
87. L. BJORK and L. A. G. HERMANNSON, *J. Am. Ceram. Soc.* **72** (1989) 1436.
88. C.-W. LI and J. YAMANIS, *Ceram. Eng. Sci. Proc.* **10** (1989) 632.
89. J. A. SALEM, S. R. CHOI, M. R. FREEDMAN and M. G. JENKINS, *J. Mater. Sci.* **27** (1992) 4421.

90. N. HIROSAKI, Y. AKIMUNE and M. MITOMO, *J. Am. Ceram. Soc.* **76** (1993) 1892.
91. J. NEIL, "Calculating Weibull Modules from Average and Standard Deviation", GTE Laboratory Report, 7/1989.
92. G. HIMSOLT and H. KNOCH, *J. Am. Ceram. Soc.* **62** (1979) 29.
93. D. R. BISWAS and R. M. FULRATH, *Trans. J. Br. Ceram. Soc.* **79** (1980) 1.
94. R. W. RICE, *J. Mater. Sci.* **19** (1984) 895.
95. A. A. STEFFEN, R. H. DAUSKARDT and R. O. RITCHIE, *J. Am. Ceram. Soc.* **74** (1991) 1259.
96. R. H. DAUSKARDT, M. R. JAMES, J. R. PORTER and R. O. RITCHIE, *ibid.* **75** (1992) 759.
97. R. W. RICE, *ibid.* **77** (1994) 2479.
98. D. E. WHITTMER and W. TRIMBLE, *Eng. Sci. Proc.* **10** (1989) 1223.
99. M. V. SWAIN and L. R. F. ROSE, *J. Am. Ceram. Soc.* **69** (1986) 511.
100. R. W. RICE, in "Advances in Ceramics", Vol. 22, "Fractography of Glasses and Ceramics", edited by J. R. VARNER and V. D. FRECHETTE (American Ceramic Society, Westerville, OH 1988) pp. 3–56.
101. K. R. McKINNEY, B. A. BENDER, R. W. RICE, and C. Cm. WU, *J. Mater. Sci.* **26** (1991) 6467.
102. K. W. WHITE and J. C. HAY, *J. Am. Ceram. Soc.* **77** (1994) 2283.
103. R. W. RICE, *ibid.* **76** (1993) 3009.
104. N. B. EDEN and J. E. BAILEY, *J. Mater. Sci*, **19** (1984) 150.
105. S. IGARASHI and M. KAWAMURA, *J. Am. Ceram. Soc.* **78(7)** (1995) 1715.
106. P. C. STRANGE and A. H. BRYANT, *J. Mater. Sci*, **14** (1979) 1863.

Received 3 October
and accepted 20 November 1995